CHAPTER 6

CHAPTER 6

Unlocking Anti-metastatic and Apoptotic Potential: Melatonin and *S. virginianum* leaf Extract Combinations in Breast Cancer Cell lines

6.1 Introduction

Metastasis stands as a formidable challenge in the fight against cancer, claiming the lives of many afflicted patients (Dillekås et al.,2019). Consequently, it has become the focal point of extensive research in both scientific and clinical spheres. While efforts have been made in unravelling the intricate molecular and cellular mechanisms underlying cancer-related mortality (Testa et al.,2019), the exact processes driving metastatic progression remain elusive, and strategies to combat metastasis remain limited. Cancer cells acquire the ability to migrate spontaneously through tissues, fuelling invasion and metastasis (Clark & Vignjevic,2015; Aguilar-Cazares et al.,2019), presenting a formidable obstacle to effective tumour management.

The migration of cancer cells plays a pivotal role in various physiological and pathological processes, including tumour development, wound healing, immunity, angiogenesis, and metastasis (Aguilar-Cazares et al.,2019; Sundaram et al.,2018; Yuan et al.,2016). The intricate regulation of cancer cell movement profoundly challenges therapeutic efforts to impede tumour progression.

Building upon the promising findings of previous chapters, which highlighted the anti-proliferative potential of *S. virginianum* leaf extracts, both alone and in combination with melatonin (Chapters 2 and 5), this study delves into the examination of phytochemicals present in *S. virginianum* leaf extracts. Through advanced separation techniques and *in silico*

analysis, specific phytochemicals have demonstrated encouraging affinities towards key cancer targets, implicating their potential efficacy in modulating cell migration, tumorigenicity and apoptotic pathways.

Aligned with these findings, the present chapter explores the anti-migratory, anti-clonogenic and apoptotic effects of S. virginianum leaf extracts and/or melatonin on MCF-7 and MDA-MB-231 cell lines. This investigation aims to shed further light on the potential therapeutic benefits of these natural compounds in combating breast cancer metastasis.

6.2 Materials and Method

In the present chapter, the experimental groups considered for the assays along with their respective concentration values, are as follows.

Table 6.2.1: Experimental group details

Experimental group	MCF-7		MDA-MB-231	
1	Control	Only complete growth media	Control	0.2% DMSO +complete growth media
2	*Sv* leaf aqueous extract : Sub IC_{50}	5 µg/mL	*Sv* leaf methanolic extract : Sub IC_{50}	6 µg/mL
3	*Sv* leaf aqueous extract : IC_{50}	10 µg/mL	*Sv* leaf methanolic extract : IC_{50}	12 µg/mL
4	Melatonin : Sub IC_{50}	12 µg/mL	Melatonin : Sub IC_{50}	24 µg/mL
5	Melatonin : IC_{50}	24 µg/mL	Melatonin : IC_{50}	48 µg/mL
6	(Extract+Melt): Sub IC_{50}	(5+12) µg/mL	(Extract+Melt) : Sub IC_{50}	(6+12) µg/mL
7	(Extract+Melt): IC_{50}	(10+24) µg/mL	(Extract+Melt) : IC_{50}	(12+24) µg/mL
8	Doxorubicin	24 µg/mL	Doxorubicin	50 µg/mL

6.2.1 Cell Morphology study

Morphological assessments of both treated and untreated MCF-7 and MDA-MB-231 cells were conducted and captured using an inverted microscope (Hill and Blask, 1988).

6.2.1.1 Experimental detail

The MCF-7 and MDA-MB-231 cell cultures were maintained as outlined in Chapter 2. These cell lines were then cultured in 6-well plates and subjected to treatment with both IC_{50} and $SubIC_{50}$ concentrations of the plant extracts, individually and in combination with melatonin, for 24 hr. Following the treatment period, the cells underwent a washing step with 1X PBS. They were subsequently observed under an inverted microscope (Olympus CKX53, Tokyo, Japan) to detect any morphological alterations induced by the treatment in the breast cancer cell lines.

6.2.2 Migration inhibition determination through Scratch Assay (Yarrow et al., 2004)

Cell migration is a fundamental process crucial for developing and maintaining multicellular organisms (Trepat et al., 2012). Aberrant cell migration is implicated in various clinical conditions, including cancer (Stuelten et al., 2018). Individual cells, cell sheets, or cell clusters traverse from one location to another during cell migration. This migration occurs in two primary forms: single-cell and collective-cell migration (De Pascalis and Etienne-Manneville, 2017). In collective cell migration, multiple cells synchronize their movements, a process regulated by cell-cell adhesion, collective cell polarization, coordination of cytoskeletal activity, and responses to chemical and mechanical cues.

6.2.2.1 Experimental detail

Based on the results of the MTT assay (Chapters 2 and 5), the chosen extracts were assessed on MCF-7 and MDA-MB-231 cell lines using IC_{50} and $subIC_{50}$ concentrations, both individually and in combination with melatonin, for the wound healing assay (Yarrow et al., 2004). MCF-7 cells were treated with the aqueous leaf extract, while MDA-MB-231 cells

were treated with the methanolic leaf extract (refer chapter 2). Initially, 1×10^5 cells/well were seeded in 12-well culture plates until a confluent monolayer formed. Subsequently, a sterile pipette tip (200 µL) was used to create a gap in the centre of each well. The cells and debris from this process were gently washed with 1X phosphate-buffered saline (PBS). Following this, the cells were exposed to the IC_{50} and subIC_{50} concentrations of the extracts. Images of the scratch area were captured at 0 hr, 6 hr, and 12 hr, using an inverted microscope (Olympus CKX53, Tokyo, Japan) at a magnification of 10X. ImageJ software was employed to analyze cell migration. The scratch closure rate was calculated using the formula: % closure = $(A^{th}/A^{t0}) \times 100$, where A^{t0} represents the scratch area at 0 hr and A^{th} denotes the scratch area at 6 hr or 12 hr.

6.2.3 Tumor formation inhibition determination through Colony formation assay (Franken et al.,2006)

Regulating tumour growth and cell migration poses a significant challenge in tumour treatment. As Franken et al. (2006) outlined, the colony formation assay was conducted to address this challenge.

6.2.3.1 Experimental detail

Viable cells from both cell lines were seeded at a density of $1x10^3$ cells/well in 6-well plates and allowed to adhere for 24 hr. Subsequently, the cells were treated with the selected extracts at IC_{50} and subIC_{50} concentrations and further incubated for 24 hr. Following incubation, the medium containing the extracts was replaced with a fresh medium, and the cells were incubated for an additional 6 days. At the end of the incubation period, the medium was removed, and the cells were washed with 1X PBS. The cells were then fixed in 500 µL of fixative solution (37% formaldehyde) for 5 min at room temperature. After fixation, the cells were stained with 10 µL of 0.5% crystal violet for 10 min at room temperature. Subsequently, the stained cells were rinsed under running tap water to remove excess dye. The visible

colonies were photographed and counted, and the survival rate was calculated as a percentage of untreated cells. This protocol follows the methodology described by Franken et al. (2006).

6.2.4 DNA Fragmentation (Kasibhatla et al.,2006)

Cell death was assessed through a qualitative DNA fragmentation assay utilising agarose gel electrophoresis. Oligonucleosomal-sized DNA fragments (180-200 bp) are widely recognized as indicators of apoptosis across various cell types (Manning & Zuzel, 2003, El-Shahawy et al.,2021). Both treated and untreated cells (Table 6.2.1) underwent DNA fragmentation analysis involving DNA isolation using the organic phase separation method, followed by agarose gel electrophoresis.

6.2.4.1 Materials

- Lysis buffer: 400mM Tris-HCl (Loba chemei #06393), 10mM EDTA (SRL #40088),150mM NaCl, 1% w/v SDS (SRL#54468) in in autoclaved dH_20
- Chloroform (SRL 96712): and Isoamyl alcohol in ration 24:1
- 70% Isopropanol (SRL 67800) in autoclaved dH_20
- 70% Ethanol (local vendor) in autoclaved dH_20

6.2.4.2 Experimental detail

MCF-7 and MDA-MB-231 cells were cultured under standard conditions, as detailed in Chapter 2. Upon reaching confluency, cells were trypsinised and transferred to 6-well plates. Following the formation of monolayers, cells were treated according to the specifications outlined in Table 6.2.1, with doxorubicin-treated cells serving as positive controls. Following the designated treatment period of 24 hr, both the cell suspension and adherent cells were collected into tubes, to which lysis buffer was added. The resulting cell lysates were then incubated at 56°C for 20 min, followed by centrifugation at 2000 rpm for 5 min. The supernatant was carefully transferred to fresh autoclaved centrifuge tubes, and chloroform:iso-amyl alcohol mixture was introduced to the supernatant. After gentle

inversion for 2-3 min, the mixture underwent centrifugation at 5000 rpm for 10 min. The resulting supernatant was transferred to another tube, and chilled isopropanol (70%) was added. After incubating at -20°C for 30 min, centrifugation was carried out at 7500 rpm for 5 min, forming a pellet. The supernatant was discarded without disturbing the pellet, which was subsequently washed with chilled 70% ethanol. Equal amounts of DNA were then subjected to agarose gel electrophoresis.

6.2.4.3 Agarose Gel Electrophoresis (Lee and Bahaman, 2010)

As outlined by Lee and Bahaman (2010), agarose gel electrophoresis facilitated DNA separation. Upon application of an electric charge, DNA molecules migrate toward the anode due to the negatively charged phosphate groups along the DNA backbone. This movement allows for the separation of DNA molecules based on size, with larger molecules travelling more slowly and smaller ones moving faster through the gel. Consequently, a Gel documentation system was used to visualize distinct bands representing various DNA fragments on the gel.

6.2.4.4 Materials

- TBE Buffer (Tris-Boric acid-EDTA) 5X: Tris buffer (54 g, SRL#71033) and boric acid extrapure (27.5 gm, SRL#80266) were dissolved in 800 mL of autoclaved distilled water and 20 mL of 0.5 M EDTA(SRL#40088) was added and final volume was made up to 1000 mL with autoclaved dH_2O.
- 1X TBE Buffer: 60 mL of 5X buffer was mixed with 200 mL of autoclaved distilled water; pH adjusted to 8.0 (using NaOH, SRL#96311) and made up to 300 mL with autoclaved dH_2O.
- Ethidium bromide (Himedia#RM813): 10mg/mL in autoclaved dH_2O
- Agarose gel: 1 gm of agarose powder (SRL#60645) was dissolved in 50 mL of 1X TBE Buffer. The solution was kept for boiling to dissolve agarose. When the solution cooled

down a bit, 2 µL ethidium bromide was added to it and casted in an electrophoretic casting plate and an electrophoretic comb was placed at an end of the gel in a way that the legs of the comb remain inside the liquefied gel. It was then allowed to solidify.

- 6X orange gel loading buffer (Himedia, Cat#ML092)
- 100 bp DNA size marker (Himedia, Cat# MBT049) & 50bp DNA size marker (Himedia, Cat# MBT084)

6.2.4.5 Experimental detail

A 2% agarose mix was prepared in 1X TBE buffer and poured into a casting tray with combs in place. The combs were carefully removed after allowing it to settle for 30 min. The gel was then fully submerged in a tank buffer. Next, 10 µL of each DNA sample was mixed with 2 µL of 6X gel-loading dye and loaded into the wells. Simultaneously, 4 µL of a DNA molecular marker, pre-loaded with gel-loading dye, was also loaded. The gel was electrophoresed at 90 V for approximately 2 hr until the dye reached the end of the gel. Subsequently, the gel was visualised under a UV transilluminator to observe the DNA fragments.

6.2.5 Nuclear morphology study: DAPI (4', 6-Diamidino-2-phenylindole) staining

The effects of plant extracts, individually and in combination with melatonin, on the nuclear morphology of cells were evaluated through DAPI staining using a fluorescent microscope. DAPI, a blue fluorescent dye, exhibits a strong affinity for the AT-rich regions of DNA in both living and fixed cells (Tarnowski et al., 1991). The assessment of nuclear morphology, particularly the presence of condensed nuclear material and fragmentation, is a crucial indicator of apoptosis (Steven et al., 2007). This technique, utilising DAPI staining, enables the discrimination between live and apoptotic cells based on their nuclear characteristics (Doonan and Cotter, 2008). Its widespread application in various studies underscores its utility in elucidating the processes underlying cell death, particularly apoptosis.

6.2.5.1 Materials

- DAPI dihydrochloride solution 1mg/ml in H_2O (SRL, #80145): Working solution was prepared 1 μg/mL using autoclaved distilled H_2O
- 37% Formaldehyde (Loba chemie,#00146)
- 1 X PBS (Himedia,#TL109)

6.2.5.2 Experimental detail

Cells of MCF-7 and MDA-MB-231 were seeded at a density of 1.5 x 10^5 cells per well in a 6-well plate. Upon monolayer formation, the cells were subjected to treatment for 24 hr. Following incubation, the cells were detached using trypsin and collected in a 1.5 mL micro-centrifuge tube. To this cell suspension, 100 μL of 37% formaldehyde solution diluted in ddH_2O was added to reach a final volume of 1 mL. After 10 min of incubation at room temperature, the cell suspension was centrifuged at 3000 rpm for 2 min. The supernatant was carefully removed without disturbing the pellet, and the cell pellet was then resuspended in 1 mL of 1X PBS. Vortexing was performed to ensure a single-cell suspension, followed by centrifugation at 3000 rpm for 2 min. The supernatant was again discarded, and the cell pellet was resuspended in 1 mL of 1X PBS containing 2 μL of DAPI solution (1 μg/mL). The cell suspension was then incubated in the dark for 20 min at room temperature. After incubation, the cell suspension was centrifuged at 3000 rpm for 2 min, and the supernatant was removed. The cell pellet was resuspended in 20 μL of 1X PBS, and a 1 μL aliquot of the suspension was transferred onto a clean glass slide. The slide was observed under a fluorescence microscope (Zeiss, U.S.A.), with excitation at 359 nm and emission at 461 nm wavelengths, to visualise DAPI-stained nuclei.

6.2.6 Annexin FITC/PI staining for apoptosis analysis using FACS

Apoptosis, the programmed cell death process, involves crucial changes in the bilayer membrane composition of eukaryotic cells, primarily composed of phospholipids such as

glycerophospholipids and sphingolipids. These alterations play a pivotal role in detecting apoptosis using flow cytometry. Annexin V is a key indicator with its affinity for phosphatidylserine (PS). Normally, PS resides on the inner side of the bilayer membrane, inaccessible to annexin V. However, PS translocate to the outer membrane during apoptosis, facilitating annexin V binding. Annexin V is conjugated with a green fluorescent dye, typically FITC, to visualise this mechanism. Consequently, cells undergoing apoptosis emit a green fluorescent signal.

Propidium iodide (PI), another crucial dye for apoptotic detection, emits a red fluorescent signal. Impermeable to the plasma membrane, PI selectively stains cells with compromised membrane integrity or those dying. Neither dye can penetrate live cells, where PS remains within the membrane. During early apoptosis, the outward translocation of PS allows annexin V-FITC binding, generating a green fluorescent signal detectable by flow cytometry. In late apoptosis, despite the persistent annexin V-FITC signal, damaged membrane integrity permits PI entry, yielding a simultaneous red signal. Thus, early apoptotic cells exhibit both green and red fluorescence.

In addition to apoptosis, some cells may undergo necrosis, characterised by abrupt cell death. Unlike apoptosis, where PS translocate to the outer membrane, necrotic cells lack this translocation. However, due to cellular damage, PI can permeate the membrane, leading to exclusive red fluorescence, indicative of cell death.

The fluorescence signals from different cell populations are plotted across four graph quadrants, facilitating the analysis of viable cells, early apoptotic cells, late apoptotic cells, and necrotic cells based on their fluorescence characteristics.

6.2.6.1 Material:

1. Apoptosis kit: Dead Cell Apoptosis Kits with Annexin V for Flow Cytometry (Invitrogen ™)

a) Annexin Binding Buffer: 5X,15 mL solution µL

b) Annexin V, Alexa Fluor 488 conjugate: 250 µL

c) Propidium iodide (PI): 100 µL

Breast cancer cell lines (MCF-7 and MDA-MB-231) were cultured in 6-well plates at a seeding density of 1.5 x 10^5 cells per well and treated with both control and experimental groups, as outlined in Table 6.2.1 for 24 hr. Following the treatment period, cells were trypsinized and centrifuged at 1200 rpm for 10 min at room temperature. The resulting cell pellet was then washed with 500 µL of chilled 1X PBS and subjected to centrifugation at 3000 rpm for 5 min. After discarding the supernatant, 500 µL of annexin binding buffer was added to each tube, followed by another round of centrifugation at 3000 rpm for 5 min. Subsequently, the supernatant was discarded, and an additional 500 µL of annexin binding buffer was added. Gently pipetting and vortexing the samples prepared a single-cell suspension.

Next, 100 µL of the cell suspension was transferred to FACS tubes, to which 5 µL of annexin and 4 µL of propidium iodide stain were added. The cell suspensions were then incubated with the dyes for 15 min at room temperature in the dark. After incubation, 400 µL of annexin V binding buffer was added to each tube and vortexed. Finally, all tubes were subjected to FACS analysis using a BD FACSCalibur instrument equipped with Cell Quest Pro Software (Version: 6.0).

6.3 Result

6.3.1 Cell morphology study

The investigation into cell morphology entailed a microscopic examination of MCF-7 and MDA-MB-231 cells across control and treated groups. Control group images (Fig. 6.3.1A, 6.3.2A) depicted cells in a healthy and confluent state. Upon treatment of MCF-7 cells with subIC$_{50}$ and IC$_{50}$ concentrations, detachment from the surface and alterations in cell morphology were evident. Notably, in the subIC$_{50}$ melatonin-treated group (Fig. 6.3.1D), cells exhibited minimal changes compared to untreated cells. Conversely, in the IC$_{50}$ melatonin-treated group, cell detachment was more pronounced than in the untreated cells.

Furthermore, combinational subIC50 and IC50 groups (Fig. 6.3.1F, 6.3.1G) displayed detached cells, and microscopic examination revealed apoptotic bodies. All images were captured at 400x magnification. Additionally, Figure 6.3.1H depicts the cellular morphology of cells treated with doxorubicin, which aligns with the experimental protocol described in the respective cited references.

In the case of MDA-MB-231 cells, those treated with subIC$_{50}$ and IC$_{50}$ concentrations (Fig. 6.3.2B and 6.3.2C) exhibited fewer instances of detachment from the surface compared to untreated control cells (Fig. 6.3.2A). Conversely, minimal changes in cell appearance were observed in the subIC50 melatonin group (Fig. 6.3.2D). However, in the IC$_{50}$ melatonin, subIC$_{50}$ combinational, IC$_{50}$ combinational group, and doxorubicin-treated cells (Fig. 6.3.2E, 6.3.2F, 6.3.2G, and 6.3.2H), alterations in cell shape were noted along with a decrease in cell numbers. The cells appeared spherical-shaped and exhibited blebbing.

These observations suggest that the treatments impacted the morphology and viability of both MCF-7 and MDA-MB-231 cells when exposed to the extract, melatonin, and their combination. The changes in cell appearance may indicate cellular stress or the activation of

specific pathways in response to the treatments. All descriptions align with the experimental findings and protocols outlined in the corresponding cited references.

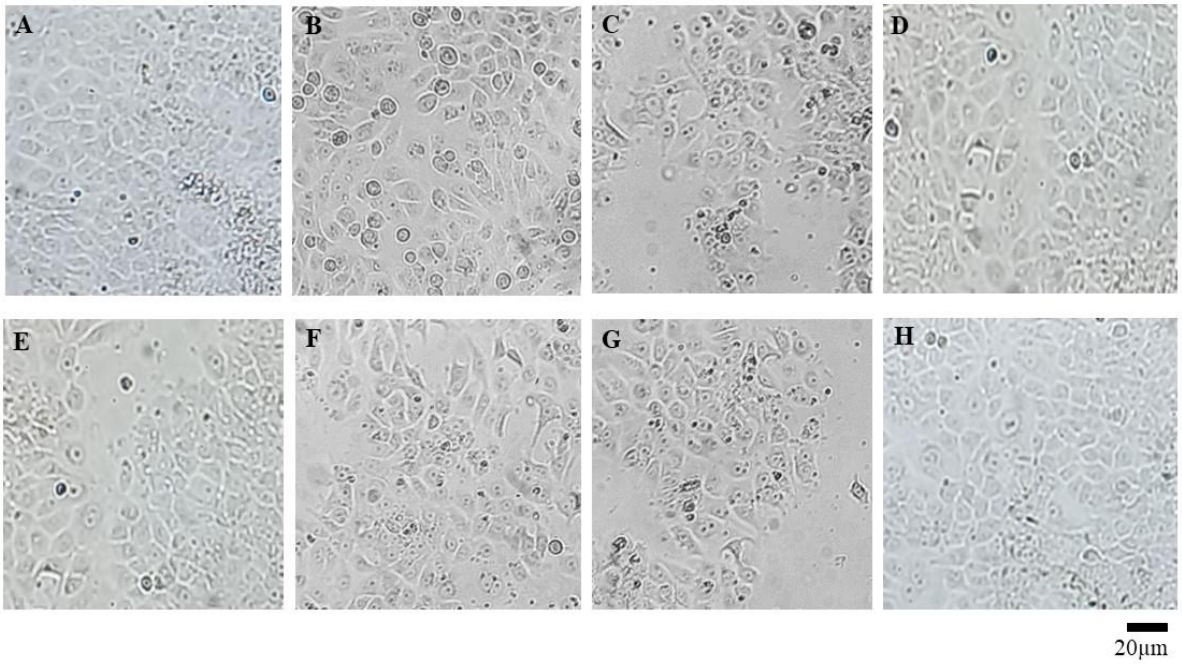

Figure 6.3.1: Cell morphology study of untreated and treated experimental groups of MCF-7 through inverted microscope.

A : Control, B : Extract Sub IC_{50} , C: Extract IC_{50} , D : Melatonin Sub IC_{50}, E : Melatonin IC_{50}, F: Extract + Mel Sub IC_{50} , G : Extract + Mel IC_{50} , H : Doxo.

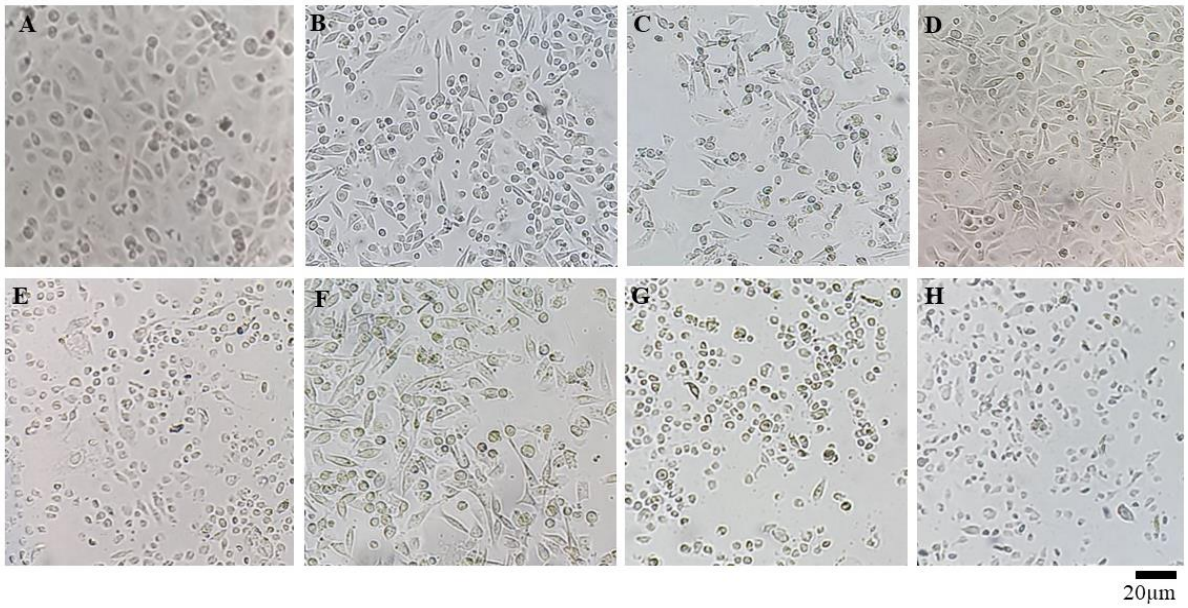

Figure 6.3.2: Cell morphology study of untreated and treated experimental groups of MDA-MB-231 through inverted microscope.

A : Control, B : Extract Sub IC_{50} , C: Extract IC_{50} , D : Melatonin Sub IC_{50} ,E : Melatonin IC_{50}, F: Extract + Mel Sub IC_{50} , G : Extract + Mel IC_{50} , H : Doxo.

6.3.2 Wound healing Assay:

In the wound healing assay, the scratch area at 0 hr for all groups was considered 100%. In the control group, cell migration decreased the scratch area percentage over time, reaching 10% at 12 hr as the wound closed. However, the scratch healing was reduced by 25% in treated cells.

The inhibition of cell migration rate at IC_{50} and $SubIC_{50}$ concentrations showed a time-dependent trend. The migration rate of MCF-7 cells exposed to 5 µg/mL aqueous leaf extract was slower, with the scratch area measuring 61% at 6 hr and 75% at 12 hr. At the IC_{50} concentration of 10 µg/mL, the scratch area was 89% at 6 hr and 79% at 12 hr, indicating a significant decrease ($p<0.01$) in cell migration rate compared to the control due to aqueous leaf extract treatment.

In individual melatonin-treated cells (Fig. 6.3.3D, 6.3.3E), the scratched area percentage was significantly higher ($p<0.01$) compared to untreated cells (Fig. 6.3A). In the combinational group (Fig. 6.3.3F, 6.3.3G), the scratch area decreased to 78% at 6 hr and 62% at 12 hr with $subIC_{50}$ concentrations of both and to 70% at 6 h and 51% at 12 hr with IC_{50} concentrations of the combination.

MDA-MB-231 cells,

6.3.3 Colony formation assay

The impact of *Sv.* aqueous leaf extract, individually and in combination with melatonin, on colony formation ability in MCF-7 and MDA-MB-231 cells were investigated to compare the difference between the colony-forming ability of treated cells versus untreated cells. The colonies are depicted in the figure 6.3.7. These findings indicate that *Sv.* aqueous leaf extract exhibited potent anti-tumour activity in both MCF-7 and MDA-MB-231 cell lines.

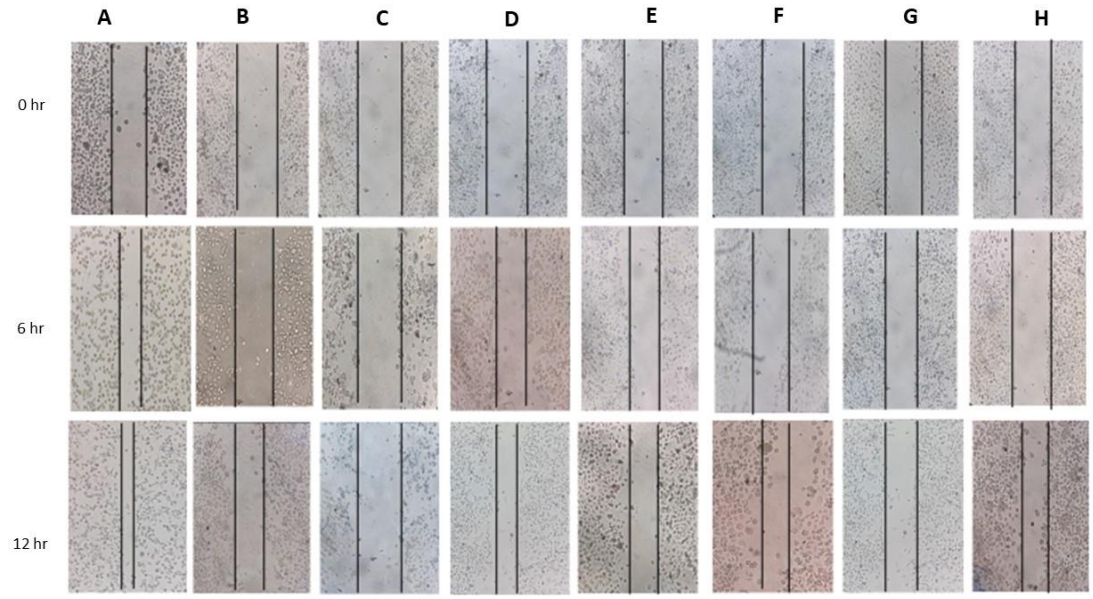

Figure 6.3.3: Present images shows the cell migration in wound area for MCF-7 cell line in different experimental groups.

A : Control, B : Extract Sub IC_{50} , C: Extract IC_{50} , D : Melatonin Sub IC_{50} ,E : Melatonin IC_{50}, F: Extract + Mel Sub IC_{50} , G : Extract + Mel IC_{50} , H : Doxo.

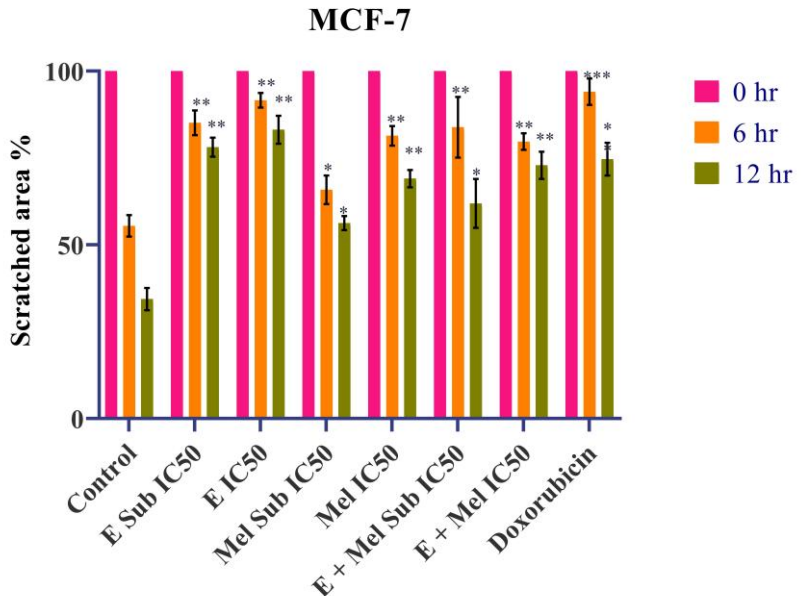

Figure 6.3.4: Scratched area % determined the cell migration inhibition activity in MCF-7 cell lines.

The data are presented as fold changes compared to untreated cells, with values represented as mean ± SEM from three individual experiments. Statistical analysis was performed using one-way ANOVA, with untreated cells as the control group. Significance levels were determined by comparing the data to untreated cells, where * represents $p < 0.05$, ** represents $p < 0.01$, and *** represents $p < 0.005$.

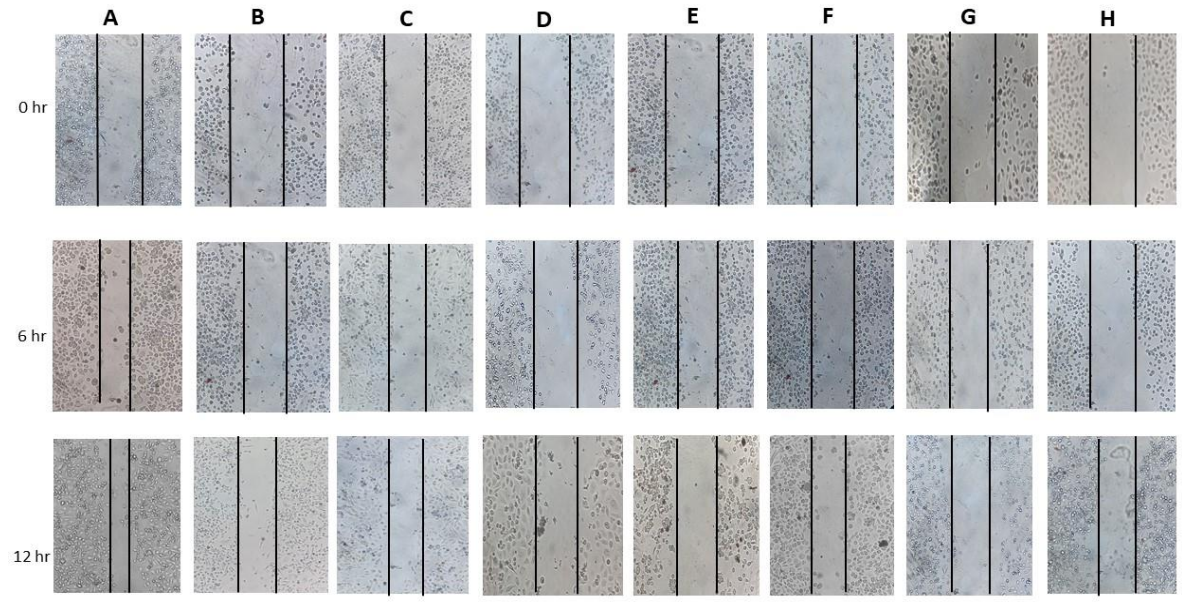

Figure 6.3.5: Present images shows the cell migration in wound area for MDA-MB-231 cell line in different groups.

A : Control, B : Extract Sub IC_{50} , C: Extract IC_{50} , D : Melatonin Sub IC_{50} ,E : Melatonin IC_{50}, F: Extract + Mel Sub IC_{50} , G : Extract + Mel IC_{50} , H : Doxo.

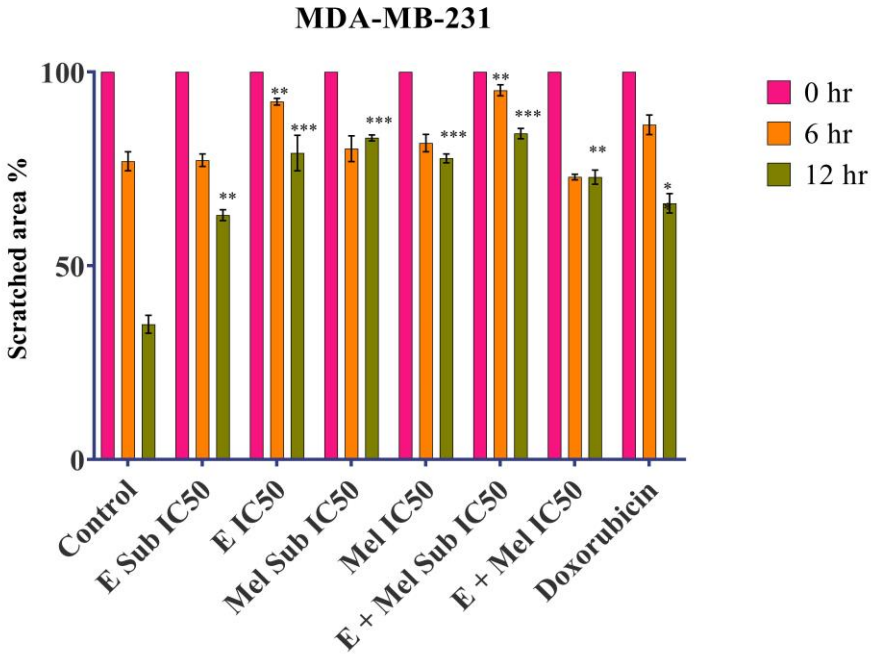

Figure 6.3.6: Scratched area % determined the cell migration inhibition activity in MDA-MB-231 cell lines.

The data are presented scratched area % in treatment groups compared to untreated cells, with values represented as mean ± SEM from three individual experiments. Statistical analysis was performed using student's t-test, with untreated cells as the control group. Significance levels were determined by comparing the data to untreated cells, where * represents $p < 0.05$, ** represents $p < 0.01$, and *** represents $p < 0.005$.

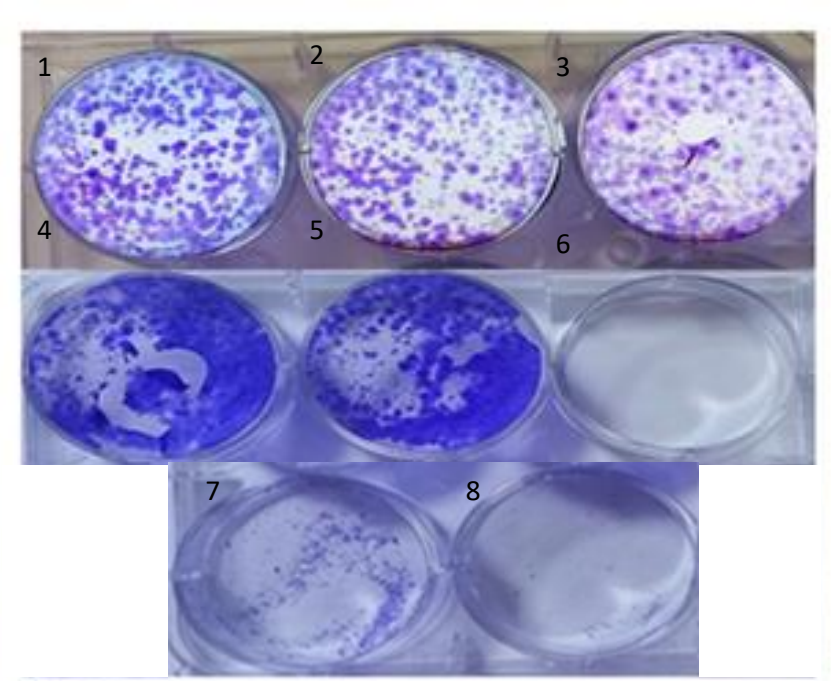

Figure 6.3.7: Colony formation determination for MCF-7

1: Control, 2: Extract Sub IC_{50} , 3: Extract IC_{50} , 4: Melatonin Sub IC_{50} , 5: Melatonin IC_{50}, 6: Extract + Mel Sub IC_{50} , 7: Extract + Mel IC_{50} , 8: Doxo.

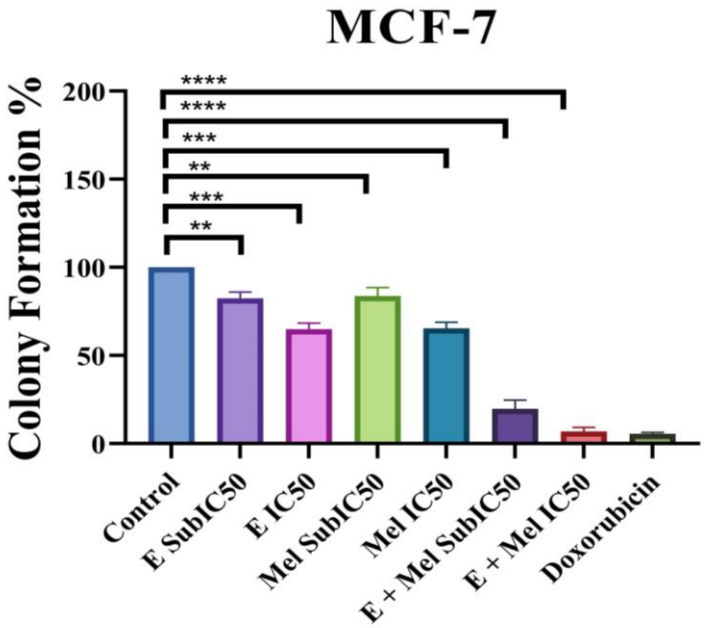

Figure 6.3.8: Graphical representation of colony formation % in MCF-7.
For each treatment, the significance was calculated in comparison to untreated cells (negative control) and positive control doxorubicin. Error bar indicates mean ± SEM from three individual experiments. Statistical analysis was performed using student's t-test, with untreated cells as the control group. Significance levels were determined by comparing the data to untreated cells, where * represents $p < 0.05$, ** represents $p < 0.01$, and *** represents $p < 0.005$.

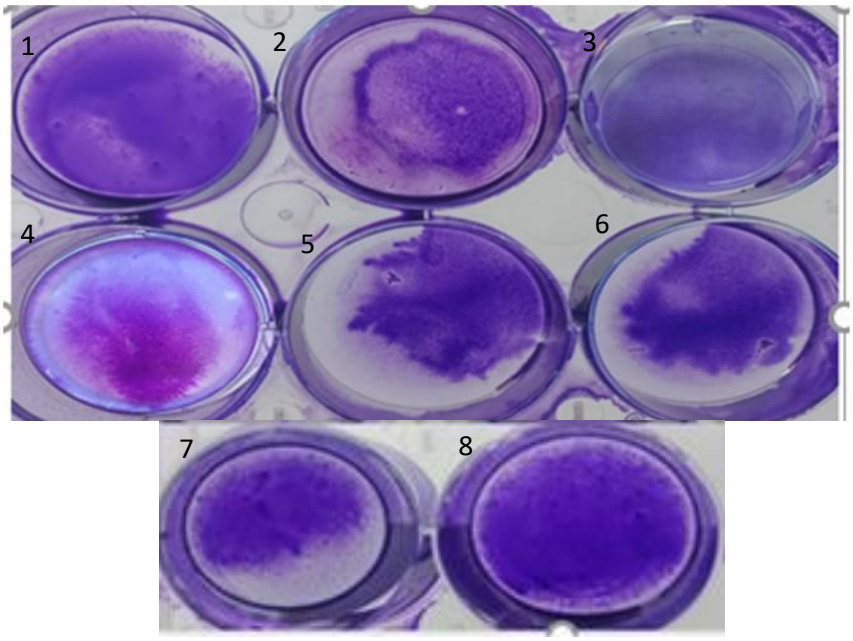

Figure 6.3.9: Colony formation determination for MDA-MB-231.

1: Control, 2: Extract Sub IC_{50} , 3: Extract IC_{50} , 4: Melatonin Sub IC_{50} , 5: Melatonin IC_{50}, 6: Extract + Mel Sub IC_{50} , 7: Extract + Mel IC_{50} , 8: Doxo.

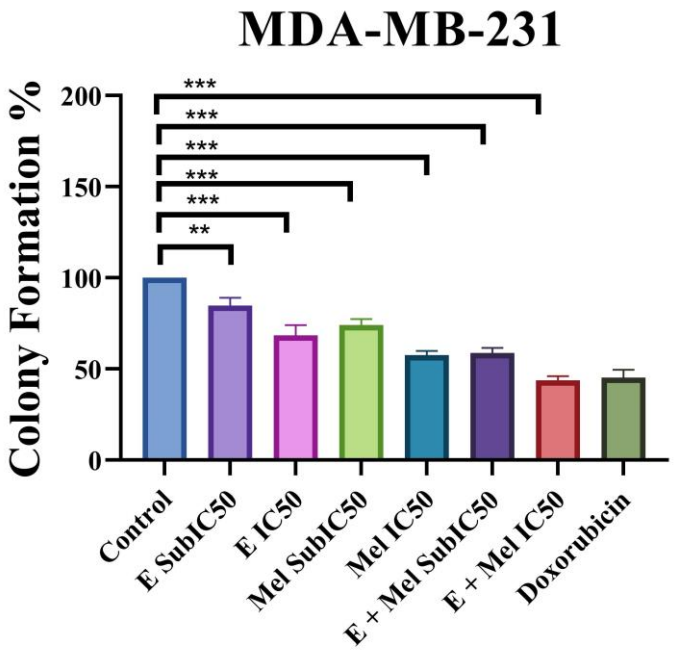

Figure 6.3.10: Graphical representation of colony formation % in MDA-MB-231.
For each treatment, the significance was calculated in comparison to untreated cells (negative control) and positive control doxorubicin. Error bar indicates mean ± SEM from three individual experiments. Statistical analysis was performed using student's t-test, with untreated cells as the control group. Significance levels were determined by comparing the data to untreated cells, where * represents $p < 0.05$, ** represents $p < 0.01$, and *** represents $p < 0.005$.

6.3.4 DNA Fragmentation Assay

DNA Fragmentation Assay is one of the most prominent assays for demonstrating apoptosis in the presence of anti-cancer compounds. In this study, *Sv* leaf extracts exhibited DNA fragmentation, individually and in combination with melatonin, in two cell lines: MCF-7 and MDA-MB-231. Figures 6.3.11 and 6.3.12 depict DNA fragments, indicated by red arrows. In MCF-7 cells, more fragments were observed in the combinational groups (Extract + Melatonin) than in the individual treatment groups. The symbol 'L' denotes the ladder (size 100kb) in both gel images.

Conversely, in MDA-MB-231 cells, all treatment groups displayed fragments with a similar pattern (Figure 6.3.12). Notably, endogenous DNase DNA degeneration, known to induce apoptosis and cleave 180-200 bp DNA fragments at nucleosome regions (Bortner et al., 1995), may contribute to the observed fragmentation. However, DNA fragments ranged from <100 kb to 400 kb in both gel images.

6.3.5 Nuclear Morphology study: DAPI staining

Figures 6.3.13 and 6.3.14 illustrate the nuclear morphology patterns observed across all experimental groups of MCF-7 and MDA-MB-231 cell lines, respectively. The arrow denotes the nuclear morphology of cells stained with DAPI within both figures.

To investigate the effects of plant extracts and melatonin on breast cancer cell lines, cells were treated with *Sv* leaf extract and/or melatonin at both IC_{50} and sub IC_{50} concentrations, administered individually and in combination, for 24 hr. The objective was to observe the patterns of chromatin condensation. Chromatin condensation was visualised in treated cells using a fluorescent microscope at a magnification of ×400. In the extract and melatonin combination group, specifically the extract + Melatonin SubIC_{50} groups, cells marked with arrows exhibited the formation of apoptotic bodies in both MCF-7 and MDA-

MB-231 cell lines. In the case of MCF-7 cells, treatment with Extract IC_{50}, Melatonin IC_{50}, and extract + Melatonin IC_{50} resulted in cell shrinkage.

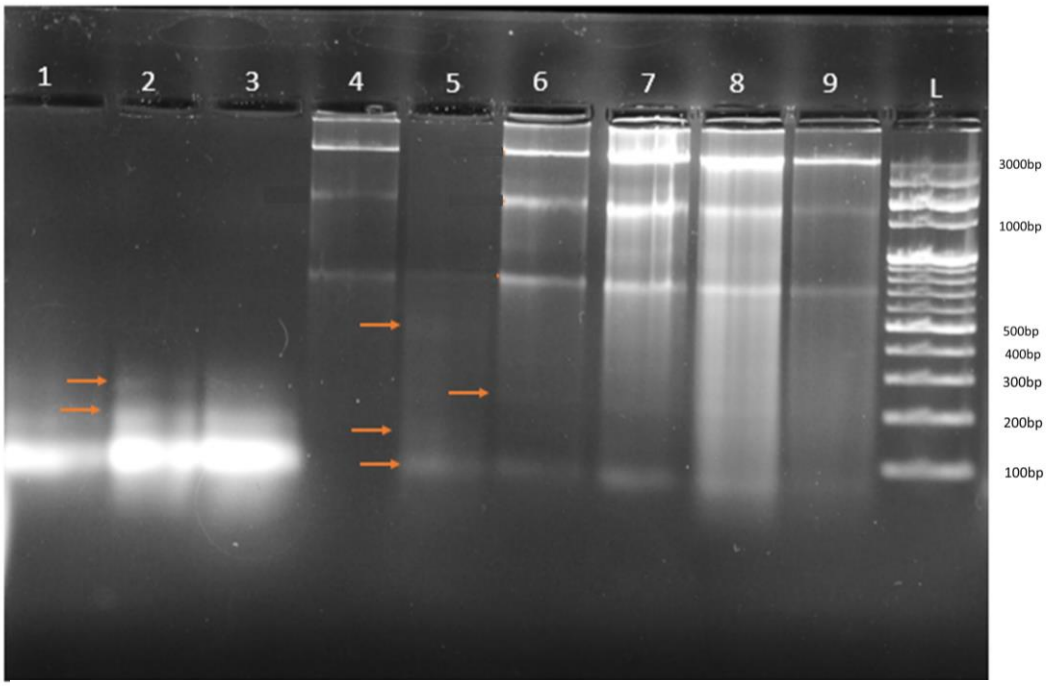

Figure 6.3.11: Agarose gel image of DNA fragmentation assay for experimental groups of MCF-7.

1: Control, 2: Extract Sub IC_{50} , 3: Extract IC_{50} , 4: Melatonin Sub IC_{50} , 5: Melatonin IC_{50}, 6: Extract + Mel Sub IC_{50} , 7: Extract + Mel IC_{50} , 8: Doxo. L : Ladder (100bp)

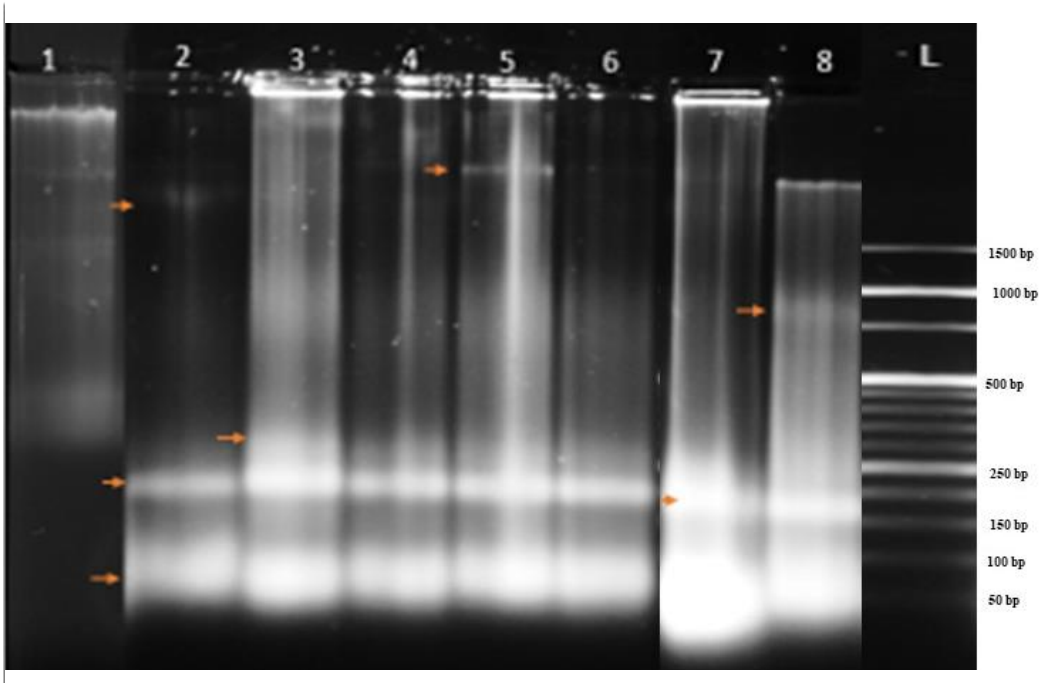

Figure 6.3.12: Agarose gel image of DNA fragmentation assay for experimental groups of MDA-MB-231.

1: Control, 2: Extract Sub IC_{50} , 3: Extract IC_{50} , 4: Melatonin Sub IC_{50} , 5: Melatonin IC_{50}, 6: Extract + Mel Sub IC_{50} , 7: Extract + Mel IC_{50} , 8: Doxo.

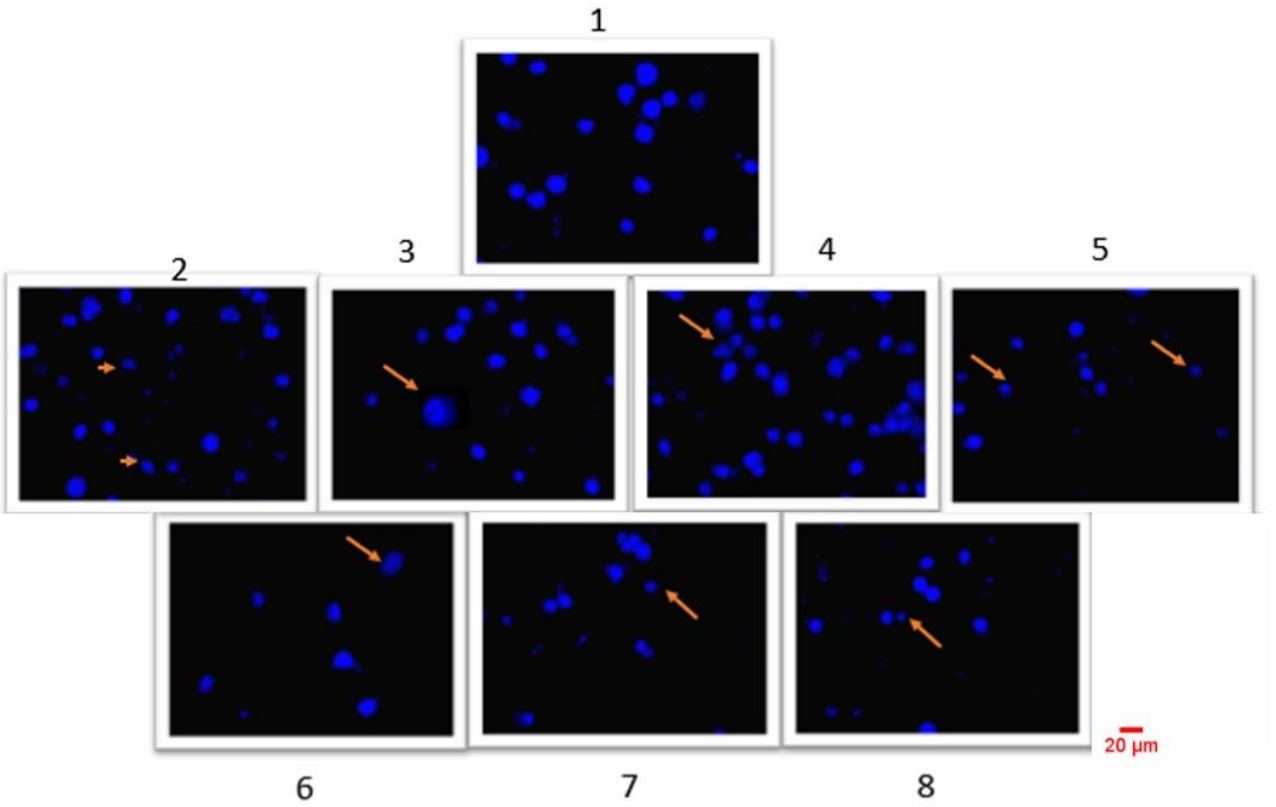

Figure 6.3.13: Nuclear morphology observational images of MCF-7 stained with DAPI (Magnification x400) using florescence microscope. The arrow shows cells having morphologically changed nucleus.

1: Control, 2: Extract Sub IC_{50} , 3: Extract IC_{50} , 4: Melatonin Sub IC_{50} , 5: Melatonin IC_{50}, 6: Extract + Mel Sub IC_{50} , 7: Extract + Mel IC_{50} , 8: Doxo.

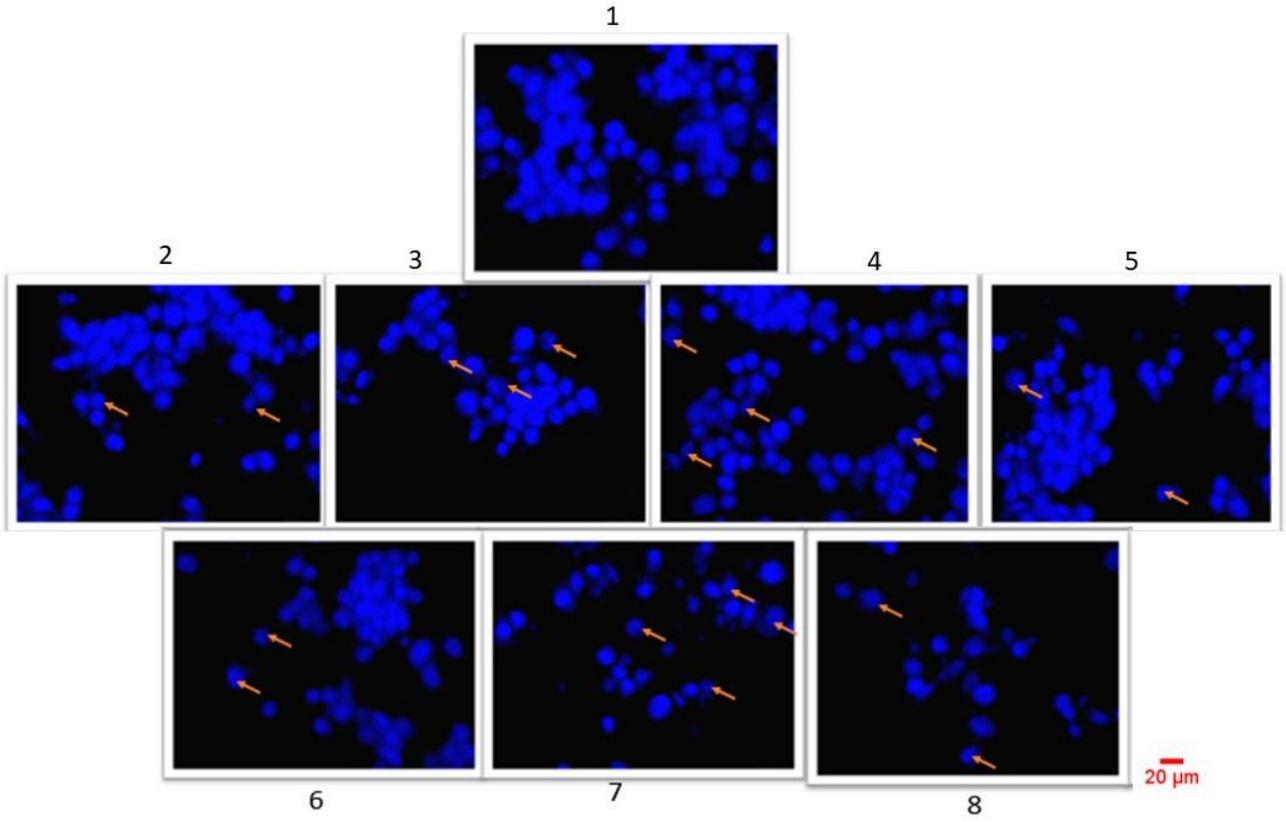

Figure 6.3.14: Nuclear morphology observational images of MDA-MB-231 cells stained with DAPI (Magnification x400) using florescence microscope. The arrow shows cells having morphologically changed nucleus.

1: Control, 2: Extract Sub IC_{50} , 3: Extract IC_{50} , 4: Melatonin Sub IC_{50} , 5: Melatonin IC_{50}, 6: Extract + Mel Sub IC_{50} , 7: Extract + Mel IC_{50} , 8: Doxo.

A

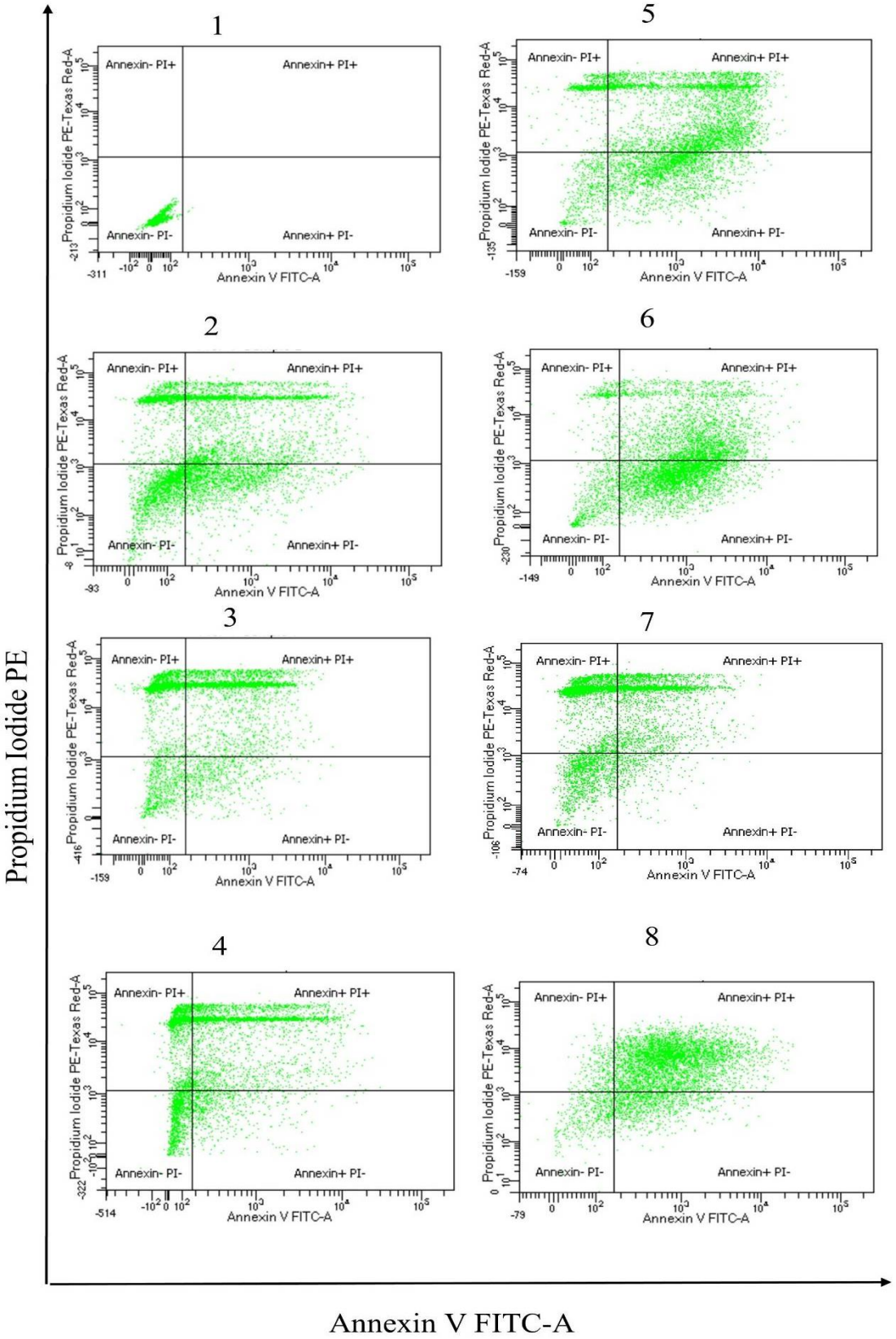

Figure 6.3.15: Flow cytometer analysis images for MCF-7 experimental groups.

1: Control, 2: Extract Sub IC_{50}, 3: Extract IC_{50} , 4: Melatonin Sub IC_{50} , 5: Melatonin IC_{50}, 6: Extract + Mel Sub IC_{50} , 7: Extract + Mel IC_{50} , 8: Doxo.

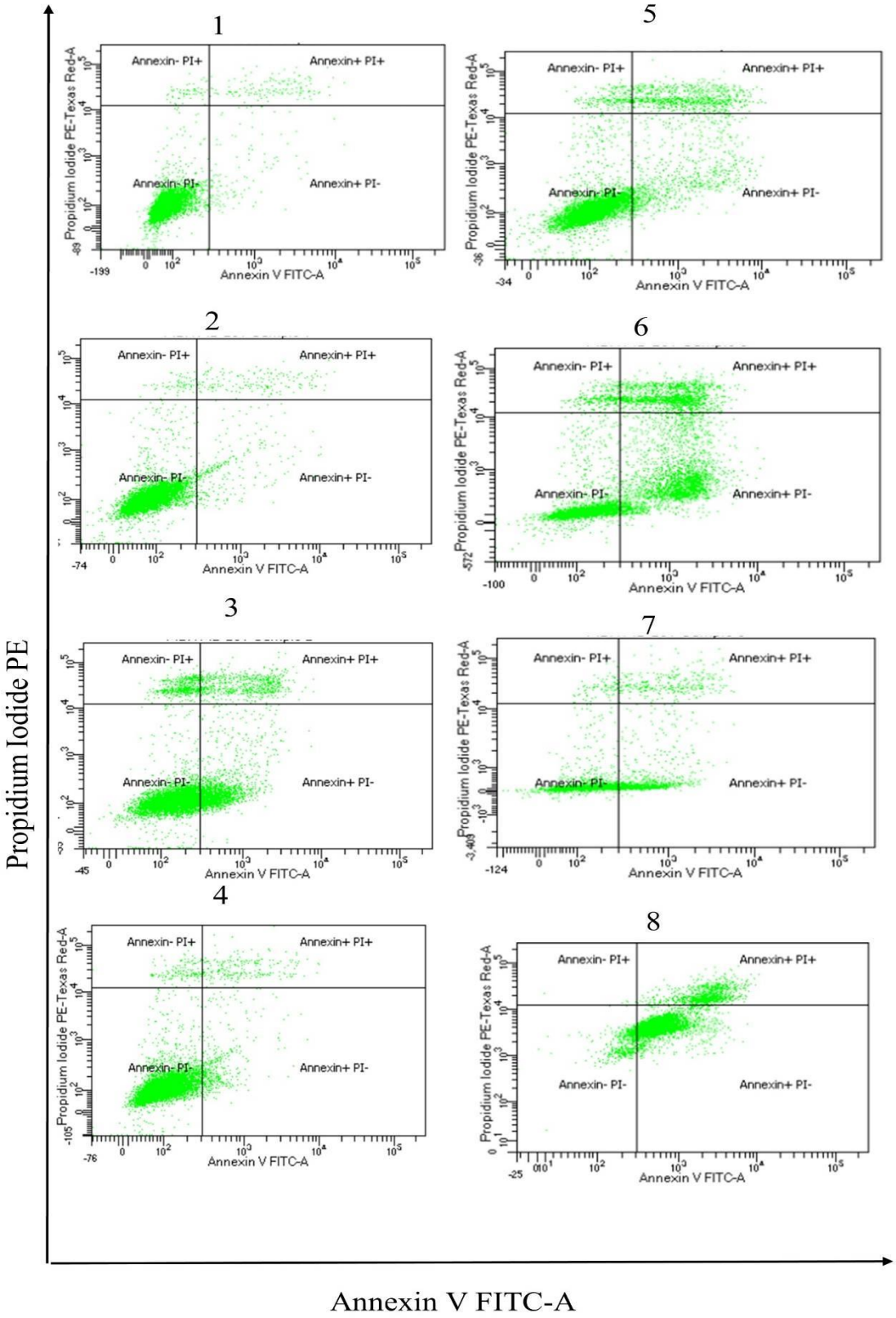

Figure 6.3.16: Flow cytometer analysis images for MDA-MB-231 experimental groups.

1: Control, 2: Extract Sub IC_{50} , 3: Extract IC_{50} , 4: Melatonin Sub IC_{50} , 5: Melatonin IC_{50}, 6: Extract + Mel Sub IC_{50} , 7: Extract + Mel IC_{50} , 8: Doxo.

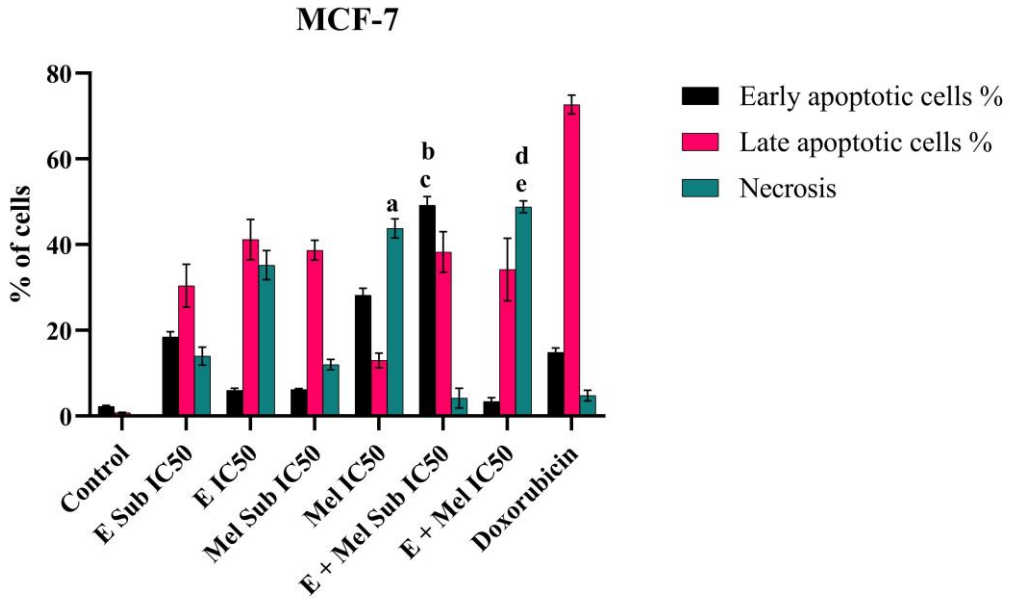

Figure 6.3.17: Graphical representation of flow cytometer analysis of MCF-7 experimental groups.

Each bar represents the % of early apoptotic, late apoptotic and necrotic cells. Error bar indicates mean ± SEM from three individual experiments. Statistical analysis was performed using one way-ANOVA. 'a' represents $p<0.001$, indicates the significance compression between Mel IC_{50} and E +Mel sub IC_{50} necrotic cells. 'b' is for early apoptotic cells % compression between E + Mel Sub IC_{50} and E IC_{50} ($p<0.001$); 'c' is for E + Mel Sub IC_{50} and Mel IC_{50} ($p<0.01$). 'd' is for necrotic cells compression between E + Mel sub IC_{50} and E + Mel IC_{50} ($p<0.001$).

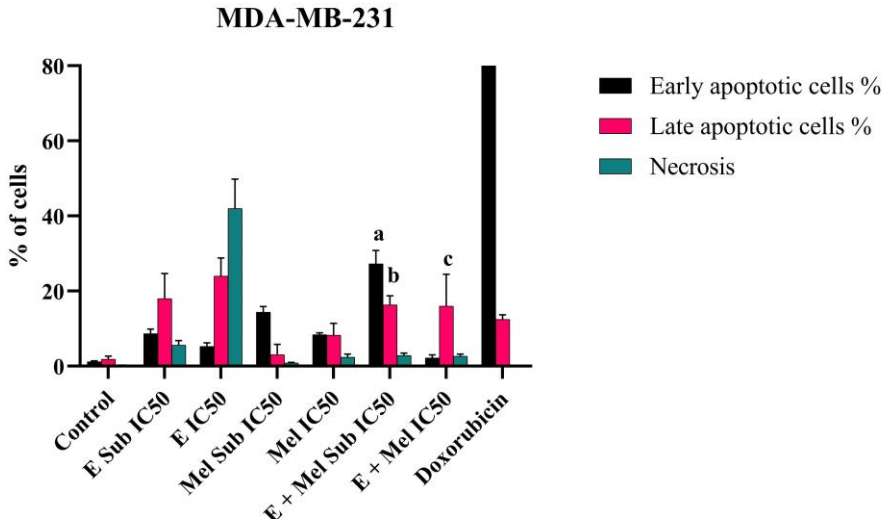

Figure 6.3.18: Graphical representation of Flow cytometer analysis of MDA-MB-231 experimental groups.

Each bar represents the % of early apoptotic, late apoptotic and necrotic cells. Each bar represents the % of early apoptotic, late apoptotic and necrotic cells. Error bar indicates mean ± SEM from three individual experiments. Statistical analysis was performed using one way-ANOVA. 'a' represents $p<0.001$, indicates the significance compression between Mel IC_{50} and E +Mel sub IC_{50} necrotic cells. 'b' is for late apoptotic cells % compression between E + Mel Sub IC_{50} and E IC_{50} (ns; 'c' is for E + Mel IC_{50} and Mel IC_{50} ($p<0.01$).

6.3.6 Apoptotic activity on breast cancer cell lines evaluated by Flow cytometer

To investigate whether cell death induced by extract and melatonin treatment leans towards apoptosis or necrosis, we employed annexin V/PI double labelling, a technique specifically geared towards identifying apoptotic cells (Figures 6.3.15 and 6.3.16). The mode of cell death was scrutinized through flow cytometry analysis utilizing annexin V-FITC/PI. The FACS analysis revealed four distinct quadrants in the images (Figures 6.3.15 and 6.3.16), with each quadrant denoting the percentage of cells of various types, as elucidated in Table 6.3.1. The percentage of cells for all experimental groups were depicted in Figure 6.3.17 for MCF-7 and Figure 6.3.18 for MDA-MB-231.

Table 6.3.1: Types of cells distributed in different quadrant in FACS analysis images

Lower left quadrant	Live cells	Annexin -/PI-
Lower right quadrant	Early apoptotic cells	Annexin +/PI-
Upper right quadrant	Late apoptotic cells	Annexin +/PI+
Upper left quadrant	Dead cells (Necrotic cells)	Annexine -/PI+

For MCF-7 cells, the FACS analysis revealed distinct patterns. In the control group (6.3.15-1), a notably higher percentage of cells remained viable compared to the treatment groups, as evidenced by their clustering in the lower left quadrant. Notably, in experimental group 6, treated with *Sv* leaf aqueous extract (sub-IC_{50}) and melatonin (sub-IC_{50}) in combination, the highest proportion of apoptotic cells was observed, constituting 49.2% of the total cell population, a statistically significant difference ($p<0.001$) when compared to experimental groups 2 and 4. Conversely, experimental group 7 exhibited a notably elevated percentage of necrotic cells (48.8%) compared to other groups.

Regarding MDA-MB-231 cells, experimental group 6 displayed the highest proportion of early apoptotic cells, comprising 27.3% of the total cell population, surpassing other groups. In contrast, the IC_{50} combinational group (group 7) exhibited cell death primarily characterised by necrosis.

The comprehensive analysis of apoptotic assays unveiled a striking outcome: when juxtaposed with individually treated groups (solely with extract or melatonin), the Sub IC_{50} combinational groups (group 6) exhibited markedly heightened apoptotic activity across both cell lines.

This chapter encapsulates a significant finding: the anti-proliferative potential of *Sv* leaf extracts, melatonin, and their combinational administration bolstered apoptosis in breast cancer cells. Building upon these discoveries, the subsequent chapter delved into molecular gene expression studies, elucidating the effects across all experimental groups through real-time PCR analysis.

6.4 Discussion

The insights provided in this chapter offer a comprehensive understanding of the effects of *Sv* leaf extract, melatonin, and their combination on breast cancer cells, particularly MCF-7 and MDA-MB-231 cell lines, concerning migration prevention, tumour growth inhibition, and apoptosis induction.

Under microscopic examination, noticeable alterations in cell morphology were observed in both MCF-7 and MDA-MB-231 cells following exposure to various treatments, either individually or in combination. At lower concentrations, minimal changes were observed, suggesting a possible protective effect against morphological alterations caused by higher concentrations. Previous studies have demonstrated melatonin's cytoprotective

properties at lower doses (Srinivasan et al., 2010). However, at IC_{50} concentrations, noticeable cell detachment occurred, indicating a dose-dependent response to melatonin treatment (Chuffa et al., 2018). When combined at sub-IC_{50} and IC_{50} concentrations in both cell lines, significant morphological alterations, such as cell detachment and the appearance of apoptotic bodies, were observed, suggesting a potential synergistic or additive effect of melatonin at various concentrations, enhancing its cytotoxicity against both types of cells. Previous research has documented similar results with combination therapies targeting cancer cells (Yang et al., 2020). Additionally, these effects align with the suggested mechanism of action of melatonin in inducing apoptosis in cancer cells (Su et al., 2017).

The wound healing assay provided valuable insights into the migratory behaviour of cancer cells in response to treatment, using the scratch area percentage as a metric to assess cell migration (Kariri et al.,2020). Both *Sv* leaf extract and melatonin led to a notable reduction in cell migration rates, with the inhibition becoming more noticeable as the concentration of the leaf extract increased, indicating a dose-dependent effect. Previous research has highlighted the anti-migratory properties of natural extracts in cancer cells (Sun et al., 2019). Similarly, the present study found that melatonin treatments, alone or in combination with the leaf extract, significantly inhibited cell migration, suggesting a synergistic effect between melatonin and the extract in impeding cancer cell motility (Su et al., 2017).

The colony formation assay, a valuable tool in cancer research, demonstrated that *Sv* leaf extract, either alone or in combination with melatonin, significantly reduced the colony-forming ability of both MCF-7 and MDA-MB-231 cells (Dong et al., 2019). This inhibition of colony formation indicates the strong anti-tumour activity of the leaf extract against MCF-7 cells and methanolic leaf extracts against MDA-MB-231 cells. The anti-tumour efficacy of

the leaf extract could be enhanced when combined with melatonin in both cell lines, suggesting a potential combinational therapeutic approach for breast cancer treatment.

In the study on DNA fragmentation, both *Sv* leaf extract and melatonin, either alone or in combination, induced DNA fragmentation in both MCF-7 and MDA-MB-231 cell lines. The combinational groups exhibited a stronger impact on DNA fragmentation in MCF-7 cells compared to individual treatments, suggesting a possible collaboration between the leaf extract and melatonin in enhancing apoptosis. However, in MDA-MB-231 cells, all treatment groups showed comparable DNA fragmentation patterns, suggesting separate effects of the leaf extract and melatonin in this cell line. Additionally, the observed variation in DNA fragment size suggests the possible contribution of endogenous DNase activity. (Cao et al., 2001).

Furthermore, nuclear morphology examination using DAPI staining revealed unique chromatin condensation patterns in treated cells, particularly in the groups receiving combined *Sv* leaf extract and melatonin at sub-IC_{50} concentrations in both cell types. Additional effects, such as cell shrinkage, were observed in groups receiving higher concentrations, indicating a dosage-dependent response to treatments (Kerr et al.1972).

Flow cytometry analysis provided quantitative data on apoptosis and necrosis in treated cell populations, offering insights into cell death mechanisms affected by *Sv* leaf extract and melatonin treatment in MCF-7 and MDA-MB-231 cell lines. The results indicated a potential synergism between extract and melatonin in promoting cell death in MCF-7 cells, with a higher proportion of necrotic cells observed in a E + Mel IC_{50} treated cells.

The analysis of flow cytometry provided valuable quantitative data on apoptosis and necrosis in the treated cell populations (Pietkiewicz, et al., 2015). The application of annexin V/PI double labelling combined with flow cytometry analysis offers valuable insights into the cell death mechanisms affected by *Sv* leaf extract and melatonin treatment in breast cancer cell lines, MCF-7 and MDA-MB-231. In the experimental group, a significant increase in apoptotic cells was observed when *Sv* leaf aqueous extract and melatonin were combined at sub-IC_{50} concentrations, particularly in MCF-7 cells. The results indicate a potential combinational action between the two treatments in promoting cell death in MCF-7 cells (Thakur et al.,2019). On the other hand, a higher proportion of necrotic cells was observed in a different experimental group, suggesting possible cytotoxic effects that may not support apoptotic cell death (Thakur et al.,2019). Similarly, in MDA-MB-231 cells, the group receiving combined treatment had the highest percentage of cells undergoing early apoptosis, while the IC_{50} combination mainly induced cell death characterised by necrosis. (Thakur et al.,2019).

Overall, the results highlight the potential of Sv leaf extract and melatonin in combination to inhibit cell migration and colony formation, induce apoptosis, and affect nuclear morphology in breast cancer cells. The combined treatment at sub-IC_{50} concentrations led to significantly increased apoptotic activity compared to individual treatments, emphasising the synergistic effects of these compounds and their potential for enhanced therapeutic outcomes when administered together.